объединенный
институт
ядерных
исследований
дубна

E15-88-864

P.Šimeček , R.Julin[1], S.Juutinen[1], M.Kortelahti[1],
J.Kumpulainen[1], D.Nosek , A.Pakkanen[1],
I.Procházka[2]

IN-BEAM STUDY OF LOW-LYING LEVELS IN THE ^{149}Sm NUCLEUS

Submitted to "Zeitschrift für Physik"

[1] Department of Physics, University of Jyväskylä, SF-40100 Jyväskylä, Finland

[2] Charles University, Prague, Czechoslovakia

1988

1. Introduction

The ^{149}Sm nucleus with N=87 lies in the lower-mass end of the deformed nuclei with A$\sim$150-180, where the shape of nuclei changes very rapidly. It is therefore an interesting object for experimental and theoretical studies. Despite many experimental works, the level scheme of ^{148}Sm is not yet clear. In the recent compilation of ref. [1], experimental data from transfer- and compound-nucleus reactions, Coulomb excitation as well as from radioactive decay of ^{149}Pm and ^{149}Eu are summarized. The experimental information on the structure of low-lying levels of ^{149}Sm originates mainly from studies of the radioactive decay as well as from studies of the ^{148}Nd(α,3nγ) and ^{150}Nd(^{3}He,4nγ) reactions. Since the most of the low-lying levels below 1 MeV of excitation energy are only weakly populated in those reactions, existing data do not contain enough information for detailed theoretical examinations. In this work the ^{146}Nd(α,nγ) reaction at E_α=16.0-20.4 MeV was used with aim to extend experimental information on nuclear structure of the low-lying non-yrast states in ^{149}Sm. The electromagnetic transition rates, evaluated from our results and the compiled data of ref. [1] are discussed in the framework of the quasiparticle-rotor model.

2. Experimental procedure and results

The data were collected by employing α-particle beams from the Jyväskylä cyclotron. Self-supporting 0.9 and 4.5 mg/cm^2 thick metallic Nd foils enriched to 97% in ^{146}Nd were used as targets.

Singles γ-ray spectra from the ^{146}Nd(α,nγ) reaction were measured using a Compton-suppressed Ge detector of NORDBALL type [2]. Measurements were performed for beam energies of E_α=16.0, 16.7, 17.4, 18.2, 18.5, 18.8 and 20.4 MeV. An example of a γ-ray spectrum obtained at 18.5 MeV is shown in Fig. 1. Resulted relative excitation-function curves for γ-transitions in ^{149}Sm are illustrated in Fig. 2. The relative intensities are normalised to the 461.9 keV γ-ray intensity. Energies and intensities for γ-rays identified to the ^{146}Nd(α,nγ)^{149}Sm reaction at E_α=18.5 MeV are given in Table 1.

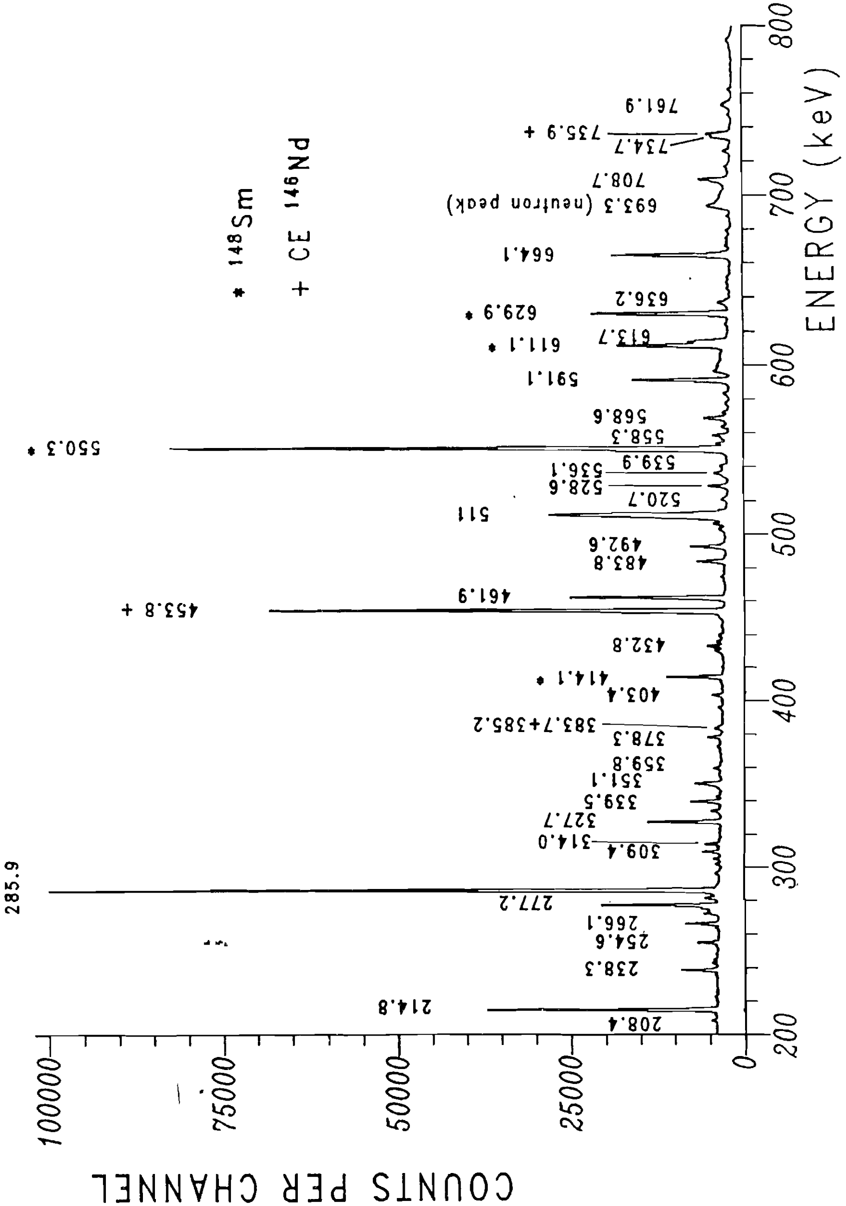

Fig. 1. Part of the singles γ-ray spectrum induced by 18.5 MeV α-particles on ^{146}Nd.

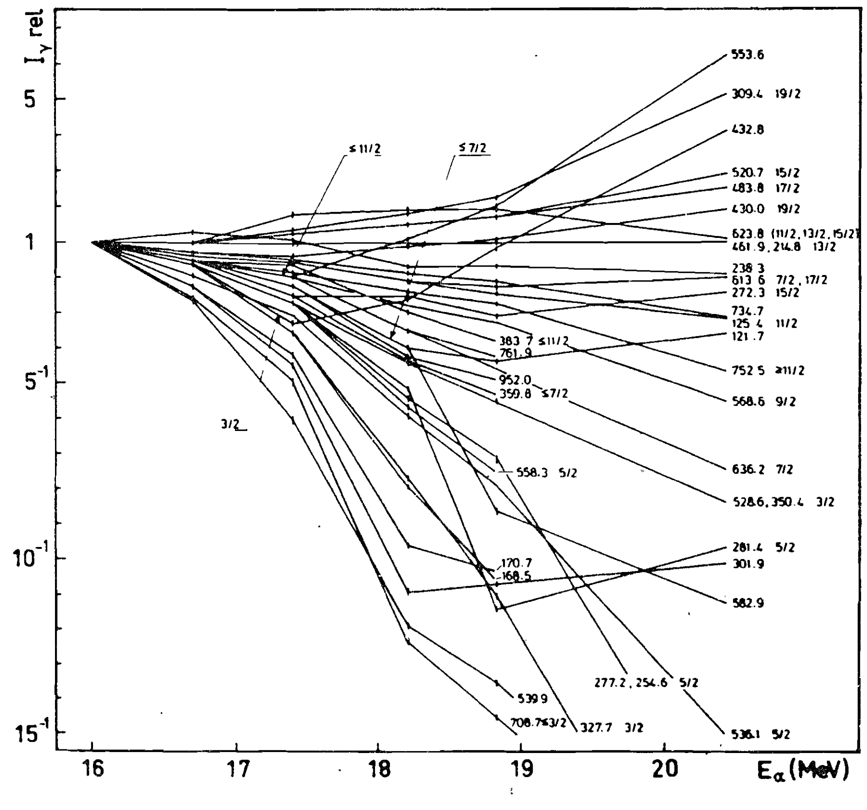

Fig.2. Relative excitation functions for some γ-rays in ^{149}Sm.

Table 1. Properties of transitions in ^{149}Sm observed in the ^{146}Nd(α,nγ)^{149}Sm reaction at E_α=18.5 MeV

E_γ[1] (kev)	I_γ	A_2/A_0	A_4/A_0	α_k ($*10^3$)	Assignments[2] $E_i \rightarrow E_f$	Com.
89.3	4.9(2)	-0.39(14)	-0.20(29)		879.0-789.7	
121.7	4.7(2)	0.19(8)	0.20(13)		399.1-277.2	
125.4	8.0(3)	0.40(38)	0.01(5)		789.7-664.3	
168.5	2.7(2)					3)
170.7	1.4(2)					3)
198.6	53.6(18)				789.7-591.1	
208.4	1.0(2)	-0.29(17)	-0.22(13)		558.3-350.3	
214.8	57.4(20)	-0.20(3)	-0.01(4)	23 (3)	879.0-664.3	
238.3	9.9(4)	0.25(5)	0.03(8)			3)
254.6	6.2(2)	0.29(2)	-0.04(3)	67(12)	277.2- 22.5	
266.1	10.1(4)	-0.79(3)	0.04(4)	71 (7)	1574.8-1308.8	
272.3	4.2(6)	-0.30(11)	-0.70(20)		1846.9-1574.8	
275.6	5.2(7)	-0.63(12)	-0.34(23)			3)
277.2	36.8(16)	-0.01(1)	0.00(2)		277.2- g.s.	
281.4	3.8(4)	0.17(17)	0.04(15)		558.3-277.2	
285.9	191[5]	-0.11(2)	-0.02(4)	67(4)	286.0- g.s.	
	32[5]				1684.2-1398.3	7)
296.1	1.7(2)					3, 6)
301.9	1.4(2)	0.43(9)	0.68(14)			3)
305.1	2.1(2)	0.60(3)	0.15 (5)	79(15)	591.1-286.0	
309.4	6.1(3)	-0.14(11)	0.09(19)		1670.6-1361.4	
314.0	6.5(3)	0.40(8)	-0.04(12)		1193.0-879.0	
327.7	30.4(11)	-0.02(1)	-0.03(2)	40.4(35)	350.3- 22.5	
339.5	12.0(5)					3)
350.4	5.0(7)				350.3- g.s	

Table 1 (cont.)

351.1	3.7(7)				636.2-286.0	
359.8	3.0(2)	0.18(10)	0.17(16)		709.9-350.3	
378.3	5.9(3)	-0.22(3)	0.01(5)		664.3-286.0	
383.7	4.1(4)				1173.4-789.7	7)
385.2	2.2(5)				1132.6-747.9	7)
403.4	4.9(4)	-0.78(8)	-0.21(15)		1193.0-789.7	
430.0	5.6(4)	0.24(6)	-0.09(10)		1670.6-1240.5	
432.8[4]	8.9(4)				709.9-277.2	^{148}Sm, 7)
435.5	4.2(3)					3)
461.9	100.0	0.355(10)	-0.112(17)	13.2(9)	747.9-286.0	
483.8	20.1(8)	0.36(16)	-0.09(3)	12(2)	1362.8-879.0	
492.6	24.6(10)	-0.23(14)	0.01(2)	7.3(9)	1240.5-747.9	
520.7	4.6(3)				1398.3-879.0	
528.6	15.5(6)				1193.0-664.3	
					528.5- g.s	
536.1	10.6(5)				558.3- 22.5	
539.9	6.0(4)					3)
553.6	9.0(15)				344.3-789.7	^{148}Sm
558.3	12.1(15)	-0.43(8)	-0.07(13)		558.3- g.s.	
563.4	4.5(14)				1926.3-1362.8	
568.6	22.2(20)	0.24(2)	0.04(4)		591.1- 22.5	
577.4	1.2(4)					3)
582.9	3.9(6)					3)
591.1	92.6(41)			6.0(9)	591.1- g.s.	CE ^{146}Nd
596.1	12.0(4)				1344.3-747.9	
613.7	37.2(15)				1361.4-747.9	
					636.2- 22.5	
623.8	2.0(5)	0.21(33)	0.31(54)		1413.6-789.7	
636.2	16.3(13)	0.14(4)	-0.19(7)		636.2- g.s.	

Table 1 (cont.)

644.9	2.6(4)				1308.8-664.3	
648.4	3.9(5)				925.6-277.2	
651.1	2.3(4)				1398.3-747.9	
656.0	2.2(7)					3)
664.1	120[5)]			4.4(9)	664.3- g.s	
	15[5)]				1413.6-747.9	
668.5	4.5(7)					3)
673.4	3.1(7)					3)
708.7	35.4(19)	0.13(2)	0.25(3)		994.5-286.0	
734.7	21.5(10)				1398.3-664.3	
752.5	8.8(12)	0.01(6)	0.06(9)		1344.3-591.3	
761.9	5.0(4)	-0.17(7)	-0.26(12)		1039.1-277.2	7)
846.2	20.4(9)				1132.6-286.0	^{56}Fe
952.0	8.4(4)	0.05(6)	-0.01(10)		1237.9-286.0	
955.4	4.5(3)					3)
1022.4	7.9(6)	-0.47(4)	0.15(7)		1308.8-286.0	

Comments

1) ±0.1 keV
2) Based on ref. [1] and present data
3) Observed in single γ-ray spectra only, no evidence for placement into level scheme of ^{149}Sm from $\gamma\gamma$ coincidence data
4) Complex peak
5) From $\gamma\gamma$ coincidence data
6) Observed in ref. [9]
7) Placed into level scheme of ^{149}Sm for first time in present work

Coincidence spectra from the ^{146}Nd(α,nγ) reaction at E_α=18.5 MeV were recorded using a 20% coaxial GeHP detector, a 15% coaxial Ge(Li) detector and a small 1.4 cm^3 planar GeHP detector in a close-geometry coincidence set-up. Resolution was about 2.1 keV at 1.3 MeV for the coaxial detectors and about 0.6 keV at 121 keV for the planar detector. The coincidence events were recorded on magnetic tapes and analyzed with a PDP 11/44 computer [3]. The $\gamma\gamma$ coincidences for ^{149}Sm are summarized in Table 2.

Table 2. The $\gamma\gamma$ coincidence observed for ^{149}Sm in ^{146}Nd(α,nγ) reaction

Gate (keV)	Coincident[1)] (keV)
89.3	125.4, 198.6, 483.8, 563.4, 591.0
121.7	(277.2)
125.4	89.3, 285.9, 383.7, 403.4, 483.8, 664.1
198.6	89.3, 285.9, 383.7, 403.4, 483.8, (553.6), 568.6, 591.0, 623.9
214.8	285.9, 314.0, 378.3, 483.8, 520.7, 563.4, 664.1
266.1	272.3, 285.9, 644.9, 664.1, 1022.8
272.1	266.1, 285.9, 1022.8
277.2	(121.7), 281.4, 358.8[1)], 432.8, 648.4, 761.9
285.9	198.6, 214.8, 266.1, 272.1, 305.1, 309.4, 351.1, 378.3, 461.9, 492.6, 596.4, 613.7, (651.1), 664.1, 708.7, 734.7, (752.5), 846.1, 952.0, 1022.8
309.4	285.9, 461.9, 613.7
314.0	198.6, 214.8, (285.9), 591.0, 664.1
327.7	208.4, 358.8
350.5	
+351.1	285.9
359.8	277.2[2)], 327.7
378.3	125.4, 214.8, 285.9
383.7	
385.2	125.4, 198.6, (285.9), 461.9
403.4	125.4, 198.6, (285.9), 591.0
430.0	(285.9), 461.9, 492.6
461.9	285.9, 309.4, (385.2), 430.0, 492.0, 596.4, 613.5, (651.1), 664.1
483.8	89.3, 125.4, 198.6, 214.8, 563.4, 591.0, 664.0
492.6	285.9, 430.0, 461.9
520.4	125.4, 198.6, 214.8
528.6	664.1
553.6	125.4, 198.6, 285.9
568.6	198.6, (403.4)
591.1	198.6, 403.4, 752.5

Table 2 (cont.)

596.4	285.9, 461.9
644.9	266.1, 664.1
648.4	277.2
613.7	285.9, 309.4, 461.9
664.3	
+665.7	125.4, 214.8, 285.9, 314.0, 461.9, 483.9, 528.6, 734.7
708.7	285.9
734.7	285.9, 664.1
752.5	285.9, 591.0
761.9	277.2
846.1	285.9
952.0	285.9
1022.8	266.1, 272.3, 285.9

Comments

1) The weak coincidence are given in paranthesess

2) Observed due to existence of the 72.5 keV transition (350.0-277.2)

Angular distributions of γ-rays were measured at the angles of 90, 110, 125, 140 and 153 degrees with respect to the beam axis. The γ-ray intensities observed at each angle were normalized by means of monitor spectra of a detector at a fixed angle. The correction coefficients for the finite solid angle were calculated by using a method of Krane [4]. Attenuation factors $\alpha_{2,4}$ were determined as smooth functions of the initial spin by assuming a pure E1 character of the 125.4, 214.8, 493.6 keV transitions and a pure E2 character of the 461.9, 568.6 keV transitions [1]. The experimental A_2/A_0 and A_4/A_0 coefficients are summarized in Table 1.

A single conversion-electron spectrum was measured at E_α=18.5 MeV using a swept-current magnetic-lens plus Si(Li) electron spectrometer [5]. A part of the conversion-electron spectrum is shown in Fig. 3. The γ-ray and conversion-electron intensities were normalized by assuming a pure E1 character of the 214.8 keV transition and a pure E2 character of the 461.9 and 550.0 keV transitions. Conversion coefficients for some transitions are presented in Table 1.

Both the angular-distribution and the conversion-electron data of the present work as well as the conversion-electron data from refs. [6, 7] were analysed to get information about the quadrupole-dipole mixing ratios of some M2/E1 and E2/M1 transitions. The results of this analysis, quantitatively determined from $A_2{}^{max}=A_2/(A_0\alpha_2)$ and $A_4{}^{max}=A_4/(A_0\alpha_4)$ values, are summarized in Table 3. The sign convention introduced in ref. [8] is accepted in our work.

Table 3. Quadrupole-dipole mixing ratios of some γ-rays populated in ^{146}Nd(α,nγ)^{149}Sm reaction

E_γ(keV)	A_2^{max}	A_4^{max}	δ(L=2/L=1)	Q=$\delta^2/(1+\delta^2)$
89.3	-0.52(20)	-0.30(40)	-0.12±0.11	0.0-5.0% E2
			or $-3.6^{+2.7}_{-1.0}$	45-96% E2
208.4	-0.68(40)	-0.60(40)	$-0.6\leq\delta\leq-0.3$	8-27% E2
214.8	-0.27(4)	-0.02(9)	0.02±0.02	0.0-0.2% M2
254.6	0.64(5)	-0.10(9)	$0.20^{+0.08}_{-0.06}$	2-7% E2
266.1	-1.07(7)	0.08(8)	-0.50±0.05	17-23% E2
272.3$^{1)}$	-0.39(15)	-1.0(5)	$-0.9\leq\delta\leq-0.5$	20-45% E2
277.2	-0.02(2)	0.00(4)	$-0.08^{+0.01}_{-0.02}$	0.5-1.0% E2
281.4$^{1)}$	0.38(22)	0.10(40)	$-0.07^{+0.22}_{-0.17}$	0.0-5.5% E2
309.4	-0.17(13)	0.10(25)	$0.07^{+0.05}_{-0.06}$	0.0-1.5% M2
314.0	0.55(15)	-0.08(27)	$-0.1\leq\delta\leq0.8$	0-40% E2
327.7	-0.06(4)	-0.08(8)	$-0.03^{+0.03}_{-0.04}$	0.0-0.5% E2
359.8	0.60(35)	0.70(70)	$0.14^{+.38}_{-0.28}$	0-21% E2
			or $2.5^{+3.8}_{-1.4}$	55-98% E2
378.3	-0.32(5)	0.02(1)	$0.00^{+0.02}_{-0.03}$	M1
403.4	-1.07(14)	-0.40(35)	$-1.9\leq\delta\leq-0.3$	8-80% E2
492.6	-0.30(18)	0.02(3)	0.00±0.09	0.0-0.1% M2
558.3	-1.0(20)	0.18(36)	$0.5\leq\delta\leq2.7$	20-88% E2
636.2	0.27(8)	-0.48(35)	$-0.30^{+0.16}_{-0.18}$	2-19% E2
1022.4	-0.69(7)	0.30(20)	$-2.8^{+0.3}_{-0.4}$	86-91% E2

Comments

1) Slope of the excitation function shows on the complex character of these peaks (see main text)

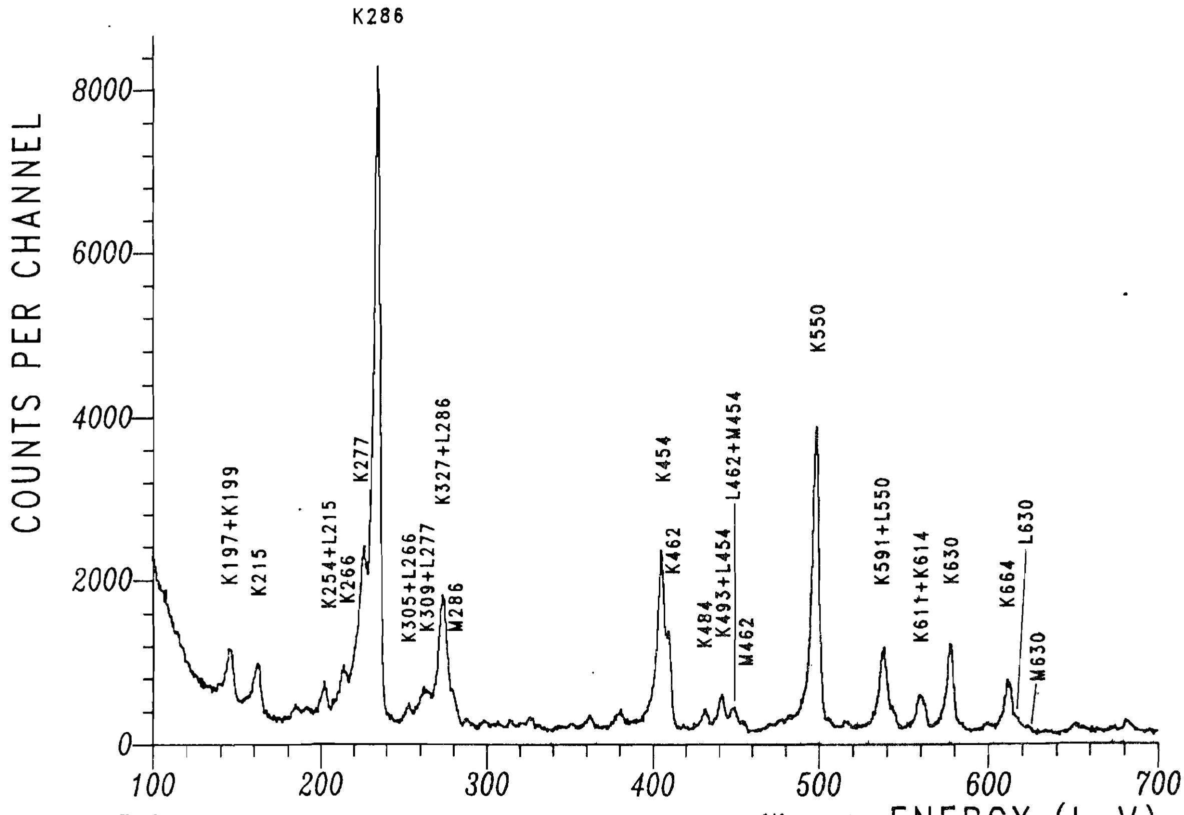

Fig.3. Part of the conversion-electron spectrum from the bombardent of ^{146}Nd with 18.5 MeV α-particles.

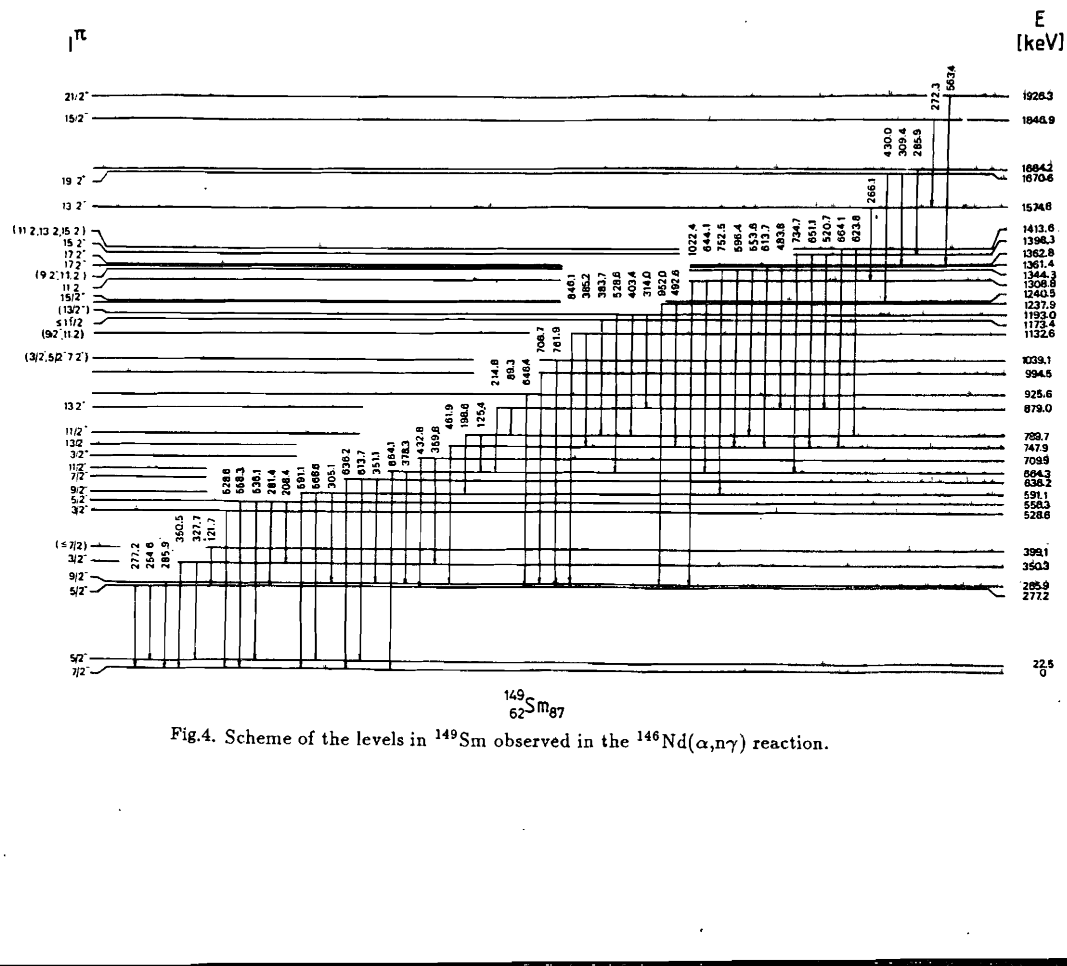

Fig.4. Scheme of the levels in ^{149}Sm observed in the ^{146}Nd(α,nγ) reaction.

3. The level scheme of ^{149}Sm

From the results described in the previous section, primarily from the $\gamma\gamma$ coincidence data, the scheme of the levels in ^{149}Sm observed in the ^{146}Nd(α,nγ) reaction was constructed. This scheme is presented in Fig. 4. Compared to the earlier works, compiled in ref. [1], in the ^{146}Nd(α,nγ)^{149}Sm reaction low-spin states in the energy region up to 1.5 MeV are more strongly populated. This allows us to draw the following conclusions:

1) The level at ~710 keV has been observed in the (d,t), (3He,α) [9,10], (d,p) [11] and (d,d') [12] reactions. The L=1,2 strength was established in these reaction studies and an assignment to $\nu p_{3/2}$, $\nu d_{3/2}$ or $\nu d_{5/2}$ configuration has been proposed for this level. Due to the strong coincidence of the 359.8 keV γ-ray with both the 327.7 and 277.2 keV (via an 72.5 keV transition) γ-rays, we have introduced a 709.9 keV level into our scheme, too. The existence of the 709.9 keV level and the new placement of the 359.8 keV transition (see refs. [1,8]) are supported by the coincidence of 277.2 and 432.8 keV γ-rays. The slopes of the excitation functions of both the 359.8 and 432.8 keV transitions at low beam energies suggest the low-spin assignment to this level. By combining our angular distribution information for the 359.8 keV γ-ray and the information of the compilation of ref. [1], we can exclude the $1/2^-$ and $5/2^-$ characters as well as determine spin and parity of $3/2^-$ for this level. The increase of the intensity of the 432.8 keV transition for E_α>17.4 MeV is due to the contribution of a γ-ray from the (α,2nγ) channel.

2) The level at ~925 keV has been observed in the (d,t) and (^{3}He,α) reactions [9,10]. According to the strong coincidence of 277.2 and 648.4 keV γ-rays in our spectra, the existence of the 925.6 keV level has been confirmed and a new 648.4 keV transition has been placed into the level scheme of ^{149}Sm.

3) The level at ~1040 keV has been observed in many transfer studies [9 – 13]. We have seen strong coincidence between 277.2 and 761.9 keV γ-rays in our spectra. Therefore, in the present level scheme we have suggested, that a 1039.1 keV level is deexcited by a new 761.9 keV transition. In agreement with the earlier transfer reaction data (L=2) the slope of the excitation function of the 761.9 keV transition implies a low spin value for this level.

4) A 952.8 keV level has been reported in an investigation of the ^{149}Pm decay [6]. However, in our experiment a 952.0 keV γ-ray is seen in coincidence with the 285.9 keV γ-ray. Furthermore, a 930.2 keV transition to the 22.5 keV level [6] has not been confirmed in our study. Therefore, we cannot confirm the 952.8 keV level, whereas the existence of a new 1237.9 keV level seems to be more probable. The slope of the excitation curve for the 952.8 keV transition implies a low-spin value for this level.

5) The slope of the excitation function of the 752.5 keV transition limits the spin value of the level at 1344.3 keV to I≤11/2. This conclusion is supported also by the excitation curve of the 553.6 keV transition at lower E_α. At higher bombarding energies a γ-ray from the (α,2n) channel apparently becomes to contribute.

Likely, the excitation pattern of the 708.7 keV transition indicates a low-spin value I ≤ 3/2 for the level at 1039.1 keV.

6) The 734.7 keV line was decomposed from the closed doublet, the second component of which originates from the ^{146}Nd coulomb excitation process. The observed excitation function of the 734.7 keV transition contradicts excitation-function data of ref. [7] as well as the present excitation pattern of the 520.7 keV transition, which is suggested to depopulate the same level at 1398.3 keV. Therefore, the spin assignment of 15/2 made in ref. [7] for this level needs a carefull experimental checking.

7) In our singles and coincidence spectra we have observed a number of new γ-rays not reported earlier. On the basis of the coincidence data some of them: 285.9 (complex peak), 383.7, 385.2, 432.8 and 623.8 keV transitions have been placed into the scheme and new levels at 1173.4 and 1684.2 keV are suggested. The slope of the excitation curve of 383.7 keV transition, which is supposed to depopulate the level at 1173.4 keV, limits the spin value for this level to I≤11/2.

The 613.6 keV line is known to be a doublet. Its components depopulate the $17/2^-$ level at 1361.4 keV and the $7/2^-$ level at 636.2 keV. The observed excitation pattern seems to be in agreement with the doublet character and the placements in the level scheme. Likely, contributions of γ-rays from the decay of higher spin levels or from other reaction channels can be seen in the 281.4 keV transition. Low-spin components are suggested for the 272.5 and 430.0 keV transitions.

Some transitions observed only in singles γ-ray spectra are presented in Table 1. On the basis of the present $\gamma\gamma$ coincidence data we cannot place these transitions to the level scheme of ^{149}Sm. However, the measured excitation curves indicate that they belong to the (α,n) channel.

4. Model calculation

It is well known that the structure of transitional nuclei in the A~150 region is very complex. The transitional character of nuclei allows many ways of approaching. The interacting-boson aproximation [14] or the extended phonon projection model [15] have been previously used in the study of electromagnetic properties of soft even-even Sm isotones. Some theoretical investigations of A~150 nuclei are based on the quasiparticle-rotor model (QRM) with inclusion of Coriolis interaction. Several attemps for description of odd Sm isotopes have already been made with varying degrees of success [7, 16, 17, 18].

To describe electromagnetic properties of low-lying levels in ^{149}Sm, populated in the ^{146}Nd(α,n) reaction, we have performed standard QRM calculations assuming the motion of independent quasiparticles in the axially deformed Nilsson potential of even-even core with δ=0.10 and parameters of pairing interaction taken from Solovjev [19]. Strong coupling between rotational and quasiparticle degrees of freedom is generated by a somewhat higher values of parameter of inertia ($\hbar^2/2J$~20 keV) used in our calculations [20]. Thus, during the optimizing procedure, while the intrinsic quasiparticle energies and parameters of inertia have been systematically varied as free parameters, the attenuation factor of η=0.9 was used for all the 16 quasiparticle states originating from the $\nu f_{7/2}$, $\nu h_{9/2}$ and $\nu i_{13/2}$ shell orbitals. For reproducing the level sequence in defined band [18], a spin dependence of the moment of inertia has been considered for three configurations, the $1/2^-$[530], $5/2^-$[523] and $7/2^-$[514] Nilsson orbitals.

Coriolis coupling of the low-energy negative parity states originating from the $f_{7/2}$ and $h_{9/2}$ orbitals, which have been previously studied in refs. [7, 16], can be demonstrated by the electromagnetic transitions presented in Table 4. In this table, reduced transition probabilities B(E2) and B(M1) and mixing ratio δ obtained in our QRM calculations, are compared to experimental values derived from experimental mixing ratios results and the compilation of lifetimes [1]. Following Hammaren [7, 16], we have classified the low-spin excitations according to their E2 decay strength to the ground state (see Fig. 5). The E2 transitions between intra shell levels, which are closely connected due to the Coriolis interaction, are remarkably strong. On the other hand, relatively weak coupling of extra shell states give the theoretical B(E2) values down to the experimental ones. A considerable discrepancy in the description of the E2 and M1 intra and/or extra shell transitions is

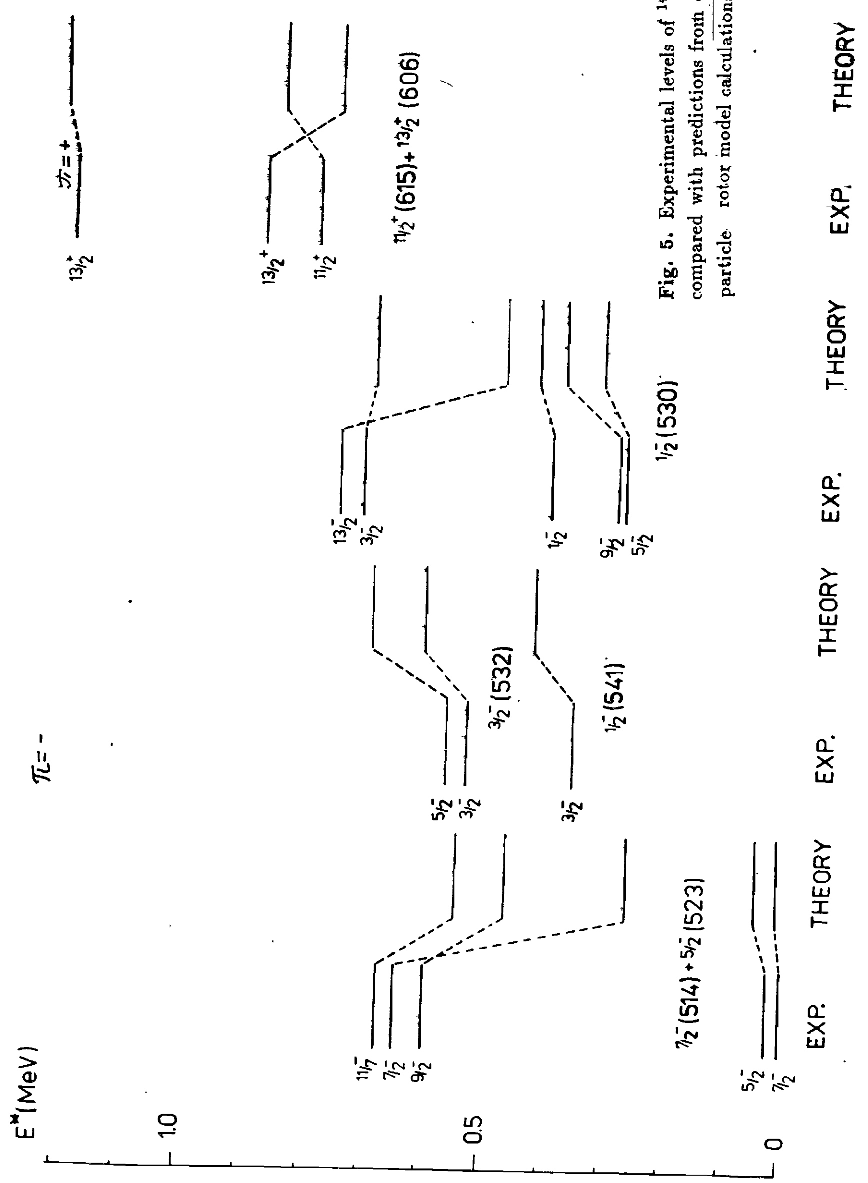

Fig. 5. Experimental levels of ^{149}Sm compared with predictions from quasi-particle rotor model calculations.

Table 4. Experimental and theoretical electromagnetic transition rates and multipole mixing ratios of transition in ^{149}Sm

E_i (keV)	J_i^π	J_f^π	E_γ (keV)	B(M1) ($*10^{-3}\mu_N^2$) exp	B(M1) theor	B(E2) (e^2fm^4) exp	B(E2) theor	$\delta(L=2/L=1)$ exp	δ theor
22.5	$5/2^-$	$7/2^-$	22.5	16(2)	16	2500(400)	1700	|0.08(1)|	0.06
277.2	$5/2^-$	$7/2^-$	277.2	≥ 6	2	≥ 4	35	$-0.08^{+0.01}_{-0.02}$	0.35
		$5/2^-$	254.6	≥ 2	12	≥ 5	55	$0.20^{+0.08}_{-0.06}$	-0.14
285.9	$9/2^-$	$7/2^-$	285.9	>7	44	<13	15	<0.11	-0.04
		$5/2^-$	263.4			6(1)	1		
350.3	$3/2^-$	$7/2^-$	350.4			860(90)	260		
		$15/2^-$	327.7	100(10)	290	0 – 70	54	$-0.03^{+0.04}_{-0.04}$	0.04
		$5/2^-$	72.9	30(3)	30	5600(2400)	129	| 0.27(6) |	0.04
528.6	$3/2^-$	$7/2^-$	528.6			270(40)	246		
		$5/2^-$	506.1	0.3(2)	144	330(60)	41	$4.9^{+0.3}_{-1.5}$	0.07
		$3/2^-$	178.3	4(1)	11	450(300)	415	| 0.5(2) |	-0.29
558.3	$5/2^-$	$7/2^-$	558.3	0.3 – 4.0	88	20 – 200	42	$0.5\leq \delta \leq 2.7$	-0.10
		$5/2^-$	536.1	3(1)	210	20 – 100	23	$-0.65^{+0.23}_{-0.43}$	0.05
		$5/2^-$	281.4	8 – 18	0.2	0 – 170	0.1	$-0.07^{+0.22}_{-0.17}$	-0.04
		$3/2^-$	208.4	8 – 20	665	300 – 1900	640	$-0.6\leq \delta \leq -0.3$	-0.05
591.1	$9/2^-$	$7/2^-$	591.1	15(10)	3	1350(50)	55	−1.5(7)	−0.65
		$5/2^-$	568.6			700(200)	215		
		$9/2^-$	305.1	10 – 18	80	0 – 220	134	0.15(15)	−0.11
636.2	$7/2^-$	$7/2^-$	636.2	>25	46	> 21	138	$-0.30^{+0.16}_{-0.18}$	0.29
		$9/2^-$	351.1	>28	7	>130	45	−0.30(10) 0.24	
664.3	$11/2^-$	$7/2^-$	664.3			1550(230)	750		
		$9/2^-$	378.3	9	38	<10	11	$0.00^{+0.02}_{-0.03}$	-0.05
879.0	$13/2^+$	$11/2^+$	89.3		1270		990	-0.12 ± 0.11	
								or $-3.6^{+2.7}_{-1.0}$	-0.02
1193.0	$13/2^+$	$11/2^+$	403.3		37		820	$-1.9< \delta <-0.3$	0.50
		$13/2^+$	314.0		3		195	$-0.1< \delta <0.8$	0.66

Parameters used in calculations [19] :

Q_0=250 e^2fm^4, e_{eff}(E2)=0.003

g_l=0.0, g_s=-2.30, g_k=0.41

most probably caused by the neglection of different core-shapes occuring in different shell excitations. Moreover, while the states originating from the $h_{9/2}$ shell seem to have almost rotational structure, those ones from the $f_{7/2}$ shell lying higher in energy can be affected by rotation-vibration coupling.

Also an attempt has been done in this paper to describe the positive parity states in the 1 MeV region of excitation as states originating from the $i_{13/2}$ orbital. The suggested interpretation imply a strong Coriolis mixing of observed $11/2^+$ and $13/2^+$ states, which is also demonstrated by approximately same B(E2) values of theoretically reduced transition probabilities between positive parity states presented in Table 4.

5. Summary

The ^{146}Nd(α,nγ) reaction appeared to be useful tool for population of the low-lying low-spin states in the ^{149}Sm nucleus. New experimental information from this reaction made it possible to newly assign some levels and to determine mixing ratios δ.

The ^{149}Sm nucleus was described in the frame of the quasiparticle-rotor model. Although the structure of the transitional weakly deformed soft nuclei seems to be much more complex than the aproach used by us, the main features of electromagnetic properties of low-spin states were quit wellreproduced.

We wish to thank cyclotron staff of the University of Jyväskylä for valuable technical assistance. One of us (P.Š.) is thankful for kind hospitality during his visits to the Department of Physics of the University of Jyväskylä.

References

[1] Szucs, J.A., Johns, M.W. and Singh, B.: Nucl.Data Sheets **49**, 1 (1985)

[2] Julin, R., Kumpulainen, J., Verho, E., Ahonen, P., Hattula, J., Juutinen, S. and Lampinen, A.: Dep. of Physics, Univ. of Jyväskylä, JYFL Annual Report 1987, p. 25

[3] Liukkonen, E., Sakkinen, M., Komppa, T., Nieminen, M. and Komu, K.: Dep. of Physics, Univ. of Jyväskylä, JYFL Annual Report 1976, p. 19

[4] Krane, K.S.: Nucl. Instr. Meth. **98**, 205 (1972)

[5] Kantele, J., Luontama, M., Passoja, A. and Julin, R : Nucl. Instr. Meth. **130**, 467 (1975)

[6] Meyer, R.,A., Meadows, J.,W.,T. and Macias, E .,S.: J.Phys. **G8**, 1413 (1982)

[7] Hammaren, E., Liukkonen, E., Piiparinen, M., Kownacki, J., Sujkovski, Z., Linblad, Th. and Ryde, H.: Nucl. Phys. **A321**, 71 (1979)

[8] Der Mateosian, E. and Sunyar, A .,W.: Atom. Data and Nucl. Data Tabl. **13**, 392 (1974)

[9] Lovhoiden, G. and Burke, D.G.: Can. J.Phys. **53**, 1182 (1975)

[10] Reckstad, J., Lovhoiden, G., Lien, J.R., Kazzaz, S.,El., Ellegaard, C., Bjerregaard, J., Knudsen, P. and Kleinheinz, P.: Nucl. Phys. **A348**, 93 (1980)

[11] Kenefick, K.A. and Sheline, R.K.: Phys. Rev. **B139**, 1479 (1965)

[12] Veje, E.: Nucl. Phys. **A103**, 188 (1967)

[13] Gales, S., Crawley, G.,M., Weber, D. and Zwiegtinski, B .: Nucl. Phys. **A398**, 19 (1983)

[14] Wolf, A. and Casten, R .,P.: Phys. Rev. **C36**, 851 (1987)

[15] Suhonen, J.: Phys. Let. **B193**, 405 (1987)

[16] Hammaren, E.: Dep. of Physics, Univ. of Jyväskylä, Res. Rep. **3** (1978)

[17] Vandenput, G. et al.: Phys. Rev. **C33**, 1141 (1986)

[18] Mäki-Kuutti, K. and Hammaren, E.: Nucl. Phys. **A411**, 125 (1983)

[19] Solovjev, V.,G.: Struktura atomnogo jadra , Nauka, Moskva (1971)

[20] Stephens, F.,S.: Rev. Mod. Phys. **47**, 43 (1975)

Received by Publishing Department
on December 15, 1988.